1951

The effective width of a circular cylindrical shell adjacent to a circumferential reinforcing rib, May 1951

B. Thurlimann

B. G. Johnston

THE EFFECTIVE WIDTH OF A CIRCULAR CYLINDRICAL SHELL ADJACENT TO A CIRCUMFERENTIAL REINFORCING RIB

Part I
Theoretical Study*

by

Bruno Thürlimann † and Bruce G. Johnston ‡

~~Fritz Engineering Laboratory~~ Report ~~213J~~

INTRODUCTION

Formulas are derived for the effective width of circular cylindrical shells reinforced by ribs in the circumferential direction. In cases where the shell can be considered to extend to infinity the effective width depends on two parameters, $\sqrt{ah}$ and $\lambda = n\sqrt{\frac{h}{a}}$. The first parameter is a function of the radius "a" and the thickness h of the shell, the second contains in addition the factor n representing the influence of the stress distribution in circumferential direction.

~~Certain~~ Simplifications, the influence of which for certain shell roof proportions was investigated and found to be insignificant, are introduced in order to present a graph for the effective width in different cases.

---

*Abridgement of a doctoral dissertation by Bruno Thürlimann submitted to Lehigh University in 1950. (Reference 12).

†Former Roberts and Schaefer Research Assistant at Fritz Engineering Laboratory, Lehigh University, Bethlehem, Pa., now Research Associate at Brown University.

‡Professor of Structural Engineering, Civil Engineering Dept., University of Michigan, formerly Director, Fritz Engineering Laboratory, Lehigh University, Bethlehem, Pa.

For the limiting case where the radius "a" of the shell increases to infinity the correspondence to the effective width of a T-Beam with a straight axis is established.

The problem of the effective width of T-Beams with a straight axis (Fig.1) was extensively investigated during the past 30 years (see Ref. (1) to (5))*. The actual stress distribution in the flange is replaced by an imaginary constant stress distribution over the effective width. Taking instead of the actual flange a flange of width equal to the effective width, the ordinary beam theory can be used to calculate the fiber stresses and the deflection of the rib. The advantages of this procedure are quite obvious.

The case of a curved T-Beam was considered by U. Finsterwalder (6), who treated the general unsymmetrical case with certain simplifications. H. Bleich (7) investigated the bending of curved knees of T- and H- sections. Th. v. Karman, (8) presented a formula for the effective width of a stiffened shell which considered the effect of only two parameters "a", and "h".

The application of cylindrical shells stiffened by ribs in a circumferential direction (Fig.2) has entered many different fields, including shell arch roofs, airplane fuselages, pressure vessels, submarines, hot metal ladles, etc. The analysis of such structures is very involved, and there seems to be a specific need for establishing the effective width of cylindrical shells adjacent to ribs in order to simplify their analysis.

*See list of references at end of report.

I. Definition of the Effective Width:

Consider a circular cylinder of radius "a" and thickness h, stiffened by a rib and subjected to arbitrary radial loads in the plane of the rib (Fig.2). The distribution of the direct forces $N_\varphi = \sigma_\varphi h$* of the shell in circumferential direction may be as shown in Fig.2, $(N_\varphi)_{x=o}$ being the direct force intensity at the rib. The width "b" of a circular ring of equal radius "a" and thickness h under the same loads is determined, under the assumption of a constant stress distribution corresponding to $(N_\varphi)_{x=o}$ over the width of the ring, so as to make the rib stresses of both structures identical.

The total circumferential force "S" produced in the shell by the action of the rib may be found by taking equilibrium for a cut φ = constant:

$$S = \int N_\varphi \, dx \qquad (1)$$

The integral is taken over the entire length of the shell. The shell of the ring must resist the same total force, (Fig.2):

$$S = b(N_\varphi)_{x=o}$$

Hence the width b of the equivalent ring is:

$$b = \frac{S}{(N_\varphi)_{x=o}} \qquad (2)$$

If the rib and cylinder are thought of as cut apart, the action of the rib upon the cylinder is equivalent to that of a string, stretched around the cylinder, as shown in Fig. 4. The string has the peculiar property of being able to act either in tension or compression. When the string force is compression, it is equivalent to a radial outward line load around the cylinder, thereby causing tangential normal forces N_φ that are tension,

* See Fig.3 and list of notations at end of report.

or positive, as shown in Fig. 3.

Likewise, the action of the shell on the rib may be thought of as due to a string carrying the same force as that applied to the cylinder, but with opposite sign. When the cylinder and the rib are joined together, the string forces cancel.

If the string force S is constant, the effect of the string is the same as that of a constant radial line load around the cylinder. In case S varies as a function of φ, tangential shear forces ($N_{\varphi x}$ in Fig.3) act on the shell in addition.

In summary, the effective width b of a cylinder is found by stretching around the cylinder a string under a string force S, calculating the direct force $(N_\varphi)_{x=o}$ directly adjacent to the string and applying Eq. (2). The imaginary T-section, composed of the rib as web and the effective width as flange, has rib stresses equal to those in the actual structure.

II. Calculation of the Effective Width:

A solution of the differential equations for cylindrical shells, acted upon by boundary forces will be summarized and the effective width will then be calculated by the above described procedure.

1. Circular Cylindrical Shell Under Boundary Forces:

In general, 10 forces and moments are necessary in specifying the equilibrium of an infinitesimal shell element of length dx and width $ad\varphi$ of a circular cylindrical shell (Fig.3). The displacements u, v and w in axial, circumferential and radial direction respectively, are shown in the same figure.

The general solution of the differential equations for arbitrary conditions at the boundaries x = constant is very complicated.* Miesel has derived an approximate solution sufficiently close for ~~any~~ practical application.** Assume a variation of the stresses in circumferential direction in form of the function cos $n\varphi$ (n being the number of complete waves) and, in addition, assume the second boundary x = l sufficiently far removed to be of no influence on the boundary x=o. Then, any unknown quantity H, where H stands for a force, moment or displacement, has the form:

$$H = \bar{H} C e^{-\mu_2 \xi} \left[k_1 \sin(\mu_1 \xi + \psi) + k_2 \cos(\mu_1 \xi + \psi) \right] \cos n\varphi \quad (3)$$

In the following Table A the most important forces, moments and displacements are given in this form. The two constants of integration are C and ψ. μ_1 and μ_2 are coefficients depending on the shell dimensions, Poisson's ratio ν and the number n of the harmonic under consideration. $\bar{H}$, k_1 and k_2 are constants depending on the quantity H. The string force S representing the sum of forces N_φ between any point x and infinity, as defined by Eq. (1) is:

$$S = S_n(x) = \int_x^\infty N_\varphi \, dx \quad (4)$$

By replacing N_φ by its value from the Table A, $S_n(x)$ becomes:

$$S_n(x) = EC\frac{2h}{k} \cdot \int_x^\infty e^{-\mu_2 \xi} \left[\frac{\mu_2}{2} \left(\mu_1^2 - \frac{1}{4}\lambda^4 \left(1 - \frac{1}{n^2}\right)(2+\nu) \right) \sin(\mu_1 \xi + \psi) + \mu_1 \left(\mu_2^2 + \frac{1}{4}\lambda^4 \left(1 - \frac{1}{n^2}\right)(2+\nu) \right) \cos(\mu_1 \xi + \psi) \right] \cos n\varphi \, dx$$

and performing the integration:

$$S_n(x) = E \frac{2ha}{k} C e^{-\mu_2 \xi} \left[-\frac{1}{4}\lambda^4 \left(1 - \frac{1}{n^2}\right)(2+\nu) \sin(\mu_1 \xi + \psi) + \mu_1 \mu_2 \cos(\mu_1 \xi + \psi) \right] \cos n\varphi \quad (5)$$

*See Ref. (9), p. 123 and Ref. (10), p. 31.

**Ref. (10), p. 48. ~~Miesel's notations were changed to conform with the ones adopted in this paper.~~

TABLE A

a radius of cylinder
h thickness of cylinder
ν Poisson's ratio for the material
n the harmonic under consideration (number of complete cosine-waves of the stresses in circumferential direction)
C, ψ constants of integration

$$\xi = \frac{x}{a}$$

$$\lambda = n\sqrt{\frac{h}{a}}$$

$$k = \frac{12a^2}{h^2}$$

$$k' = k\left[1 + \frac{1}{2}\lambda^4\left(1 - \frac{1}{n^2}\right)\right]$$

$$\mu_1 = \sqrt[4]{3}\sqrt{\frac{a}{h}}\sqrt{\sqrt{1 + \frac{1}{2}\lambda^4\left(1 - \frac{1}{n^2}\right)} - \frac{1}{\sqrt{3}}\lambda^2}$$

$$\mu_2 = \sqrt[4]{3}\sqrt{\frac{a}{h}}\sqrt{\sqrt{1 + \frac{1}{2}\lambda^4\left(1 - \frac{1}{n^2}\right)} + \frac{1}{\sqrt{3}}\lambda^2}$$

H	$\overline{H}$	k_1	k_2
$E\frac{\partial w}{\partial x}$	$-E$	1	0
N_x	$Eh\left(\frac{1}{k} + \frac{n^2-1}{k'}\right)$	μ_2	$-\mu_1$
N_φ	$E\frac{2h}{k}$	$\mu_2\left[\mu_1^2 - \frac{1}{4}\lambda^4\left(1 - \frac{1}{n^2}\right)(2+\nu)\right]$	$\mu_1\left[\mu_2^2 + \frac{1}{4}\lambda^4\left(1 - \frac{1}{n^2}\right)(2+\nu)\right]$
M_x	$E\frac{ah}{k}$	$\mu_2\left(1 - \frac{n^2\nu}{\sqrt{k'}}\right)$	$-\mu_1\left(1 + \frac{n^2\nu}{\sqrt{k'}}\right)$
M_φ	$E\frac{ah}{k}$	$\mu_2\left(\nu - \frac{n^2}{\sqrt{k'}}\right)$	$-\mu_1\left(\nu + \frac{n^2}{\sqrt{k'}}\right)$
$S_n(x)$	$E\frac{2ah}{k}$	$-\frac{1}{4}\lambda^4\left(1 - \frac{1}{n^2}\right)(2+\nu)$	$\mu_1 \cdot \mu_2$

General Case:

$$H = \overline{H} C e^{-\mu_2 \xi}\left[k_1 \cdot \sin(\mu_1 \xi + \psi) + k_2 \cdot \cos(\mu_1 \xi + \psi)\right]\cos n\varphi$$

Special Case:

$$M_x = E\frac{ah}{k} C e^{-\mu_2 \xi}\left[\mu_2\left(1 - \frac{n^2\nu}{\sqrt{k'}}\right)\sin(\mu_1 \xi + \psi) - \mu_1 \cdot \left(1 + \frac{n^2\nu}{\sqrt{k'}}\right)\cos(\mu_1 \xi + \psi)\right]\cos n\varphi$$

To the tangential shear force in circumferential direction $N_{x\varphi}$ (see Fig.3), the twisting moment $M_{x\varphi}$ contributes a component $\frac{1}{a} M_{x\varphi}$. Expressed as a function of the string force $S_n(x)$, the total tangential shear force T becomes:

$$T = N_{x\varphi} + \frac{1}{a} M_{x\varphi} = \frac{1}{a} \frac{\partial S_n(x)}{\partial \varphi} \qquad (6)$$

This shear force T ~~must be used~~ is the basis of for designing the diagonal steel in reinforced concrete shells adjacent to stiffeners.

2. Effective Width of an Infinitely Long Cylinder (Poisson's ratio $\nu \cong 0$)

The following derivations are greatly simplified if Poisson's ratio ν is taken equal to zero. The influence of this simplification is insignificant for concrete. In the case of steel ($\nu = 0.3$) the error involved amounts to only 2.5%.

In the middle part of a infinitely long cylinder a string force S is applied (Fig.4). S can have any variation, and may be represented by a Fourier series. The effective width will be derived for the n^{th} term of this series. Consider the unit string force:

$$S = S_n \cos n\varphi = 1 \cos n\varphi \qquad (7)$$

Each of the two parts on both sides of the string will carry half of this string force. The continuity for the two parts requires that the slope in x-direction at $x = 0$ is zero. By using Table A the two conditions take the form:

$$x = 0: \quad S_n(0) = E\,\frac{2ah}{k}\,C\mu_1\mu_2 \cos\psi \cos n\varphi = \frac{1}{2}\cos n\varphi$$

$$E\,\frac{\partial w}{\partial x} = -EC \sin\psi \cos n\varphi = 0$$

The second of these equations requires $\psi = 0$ and the other constant of integration becomes:

$$\left.\begin{aligned} C &= \frac{1}{4}\,\frac{k}{Eah\mu_1\mu_2} \\ \psi &= 0 \end{aligned}\right\} \quad (8)$$

N_φ is calculated by replacing in Table A the two constants C and ψ by the expressions (8):

$$(N_\varphi)_{x=0} = \frac{1}{2a\mu_2}\left[\mu_2^2 + \frac{1}{2}\lambda^4 \cdot \left(1 - \frac{1}{n^2}\right)\right] \cos n\varphi \quad (9)$$

The effective width is the ratio of the applied string force S to the direct Force N_φ per unit width at x = 0. (Eq. (2)):

$$b = \frac{S}{(N_\varphi)_{x=0}} = \frac{2a}{\mu_2\left[1 + \dfrac{\lambda^4\left(1 - \frac{1}{n^2}\right)}{2\mu_2^2}\right]}$$

If μ_2 is replaced by its value given in Table A,

$$b = 1.52\sqrt{ah}\,\frac{1}{\sqrt{\sqrt{1 + \frac{1}{2}\lambda^4\left(1 - \frac{1}{n^2}\right) + \frac{1}{\sqrt{3}}\lambda^2}}} \cdot \frac{1}{1 + \dfrac{\lambda^4\left(1 - \frac{1}{n^2}\right)}{2\mu_2^2}} \quad (10)$$

In case of axial symmetry the number n of the waves of the string force S around the cylinder is zero (string force S is constant). $\lambda = n\sqrt{\frac{h}{a}}$ being proportional to n

will be zero too, and Eq. (10) reduces to:

$$\lambda = 0: \qquad \underline{\underline{b = 1.52\sqrt{ah}}} \tag{11}$$

Eq. (10) is essentially a function of the two parameters $\sqrt{ah}$ and λ. It can be shown that in practical applications ($\frac{h}{a} < \frac{1}{5}$; $\frac{nh}{a} < \frac{1}{2}$) the terms $\frac{1}{n^2}$ and $\lambda^4(1-\frac{1}{n^2})$ may be safely neglected.* Then the effective width becomes:

$$b = 1.52\sqrt{ah}\;\frac{1}{\sqrt{\sqrt{1+\frac{1}{2}\lambda^4}+\frac{1}{\sqrt{3}}\lambda^2}} \tag{12}$$

which is an expression in terms of the two parameters $\sqrt{ah}$ and λ only. For the purpose of tabulating Eq. (12) the following form is chosen:

$$\underline{\underline{b = K\cdot\sqrt{ah}}} \tag{12a}$$

$$K = \frac{1.52}{\sqrt{\sqrt{1+\frac{1}{2}\lambda^4}+\frac{1}{\sqrt{3}}\lambda^2}} \tag{12b}$$

Fig. 5 is a graph representing the coefficient K for the present ($\beta l = \infty$) and several other cases as a function of λ. Note the rapid decrease of the effective width by increasing λ.

---

* See Ref. (12), p. 37 for an investigation of this simplification.

The cross bending stress σ_x under the rib will be calculated. The bending moment M_x at $x = 0$ is: (Table A and Eq. (8))

$$(M_x)_{x=0} = -\frac{1}{4\mu_2}\cos n\varphi \qquad (13)$$

Computing the bending stress σ_x and the direct stress σ_φ (Eq. (9)) the ratio of the two stresses becomes:

$$\left|\frac{\sigma_x}{\sigma_\varphi}\right|_{x=0} = \frac{6M_x}{hN_\varphi} = \frac{3a}{h\left[\mu_2^2+\frac{1}{2}\lambda^4\left(1-\frac{1}{n^2}\right)\right]}$$

$$\left|\frac{\sigma_x}{\sigma_\varphi}\right|_{x=0} = \frac{1.7321}{\left(\sqrt{1+\frac{1}{2}\lambda^4\left(1-\frac{1}{n^2}\right)}+\frac{1}{\sqrt{3}}\lambda^2\right)} \cdot \frac{1}{1+\frac{\lambda^4\left(1-\frac{1}{n^2}\right)}{2\mu_2^2}}$$

Using the same simplifications as for Eq. (10)

$$\left|\frac{\sigma_x}{\sigma_\varphi}\right|_{x=0} = \frac{1.7321}{\sqrt{1+\frac{1}{2}\lambda^4}+\frac{1}{\sqrt{3}}\lambda^2} \qquad (14)$$

The use of Eq. (14) is quite obvious. It gives with a minimum of calculation the maximum cross bending stress σ_x if the the direct stress σ_φ is known. Note that

for axially symmetrical loads ($n = \lambda = 0$), the maximum cross bending stress is 1.73 times the stress σ_φ .

3. Effective Width at or Near the End of a Semi-infinite Cylinder:

A unit string force $S=1 \cos n\varphi$, making n complete cosine-waves around the circumference, is applied to the end of a semi-infinite cylinder. The boundary conditions for the free end x=o are ,

$$\left.\begin{aligned} x=o: \quad S_n(0) &= 1 \cos n\varphi \\ M_x &= 0 \end{aligned}\right\} \qquad (15)$$

The derivation of the effective width follows a pattern similar to that previously outlined for the infinite cylinder and the following expression is arrived at:

$$b = 0.38 \sqrt{ah} \; \frac{1}{\sqrt{\sqrt{1 + \frac{1}{2}\lambda^4} + \frac{1}{\sqrt{3}}\lambda^2}} \left[1 + \frac{\lambda^2}{3\sqrt{1 + \frac{1}{2}\lambda^4}} \right] \qquad (16)$$

Using the form:

$$\underline{\underline{b = K \sqrt{ah}}} \qquad (16a)$$

where:

$$K = \frac{0.38}{\sqrt{\sqrt{1 + \frac{1}{2}\lambda^4} + \frac{1}{\sqrt{3}}\lambda^2}} \left[1 + \frac{\lambda^2}{3\sqrt{1 + \frac{1}{2}\lambda^4}} \right] \qquad (16b)$$

values of K for different values of λ are given in the graph of Fig. 5 (case $\beta l = 0$). The effective width is readily determined by use of this diagram.

For axial symmetry ($n = \lambda = o$), Eq. (16) reduces to:

$$\underline{\underline{b = 0.38 \sqrt{ah}}} \qquad (17)$$

The ratio of the maximum cross bending stress σ_x (at a certain distance from the free end x=o) to the direct stress σ_φ at x=o, for the case of axial symmetry, is:

$$\lambda=0: \quad \left| \frac{\sigma_x}{\sigma_\varphi} \right|_{max} = 0.56$$

With increasing λ this ratio decreases rapidly

($\lambda = 1$; $\left|\frac{\sigma_x}{\sigma_\varphi}\right| = 0.30$)

The solution of the effective width for a cylinder extending on one side of the rib to infinity* and having a finite overhang l on the other side ($0 \leq l \leq \infty$) is obtained (Ref. 12) by superposition of the two cases given herein, (infinitely long and end of semi-infinite cylinder) is shown. Length limitations do not permit inclusion of details but the results are presented graphically in Fig. 5.

4. Discussion of the Equations for the Effective Width:

In the case of axial symmetry, the effective width b by Eq. (11) or (17) is solely a function of $\sqrt{ah}$. "b" depends on the ability of the shell to "escape" radially by (displacement w). The factor $\sqrt{ah}$ describes this property. In the general case, the parameter $\lambda = n\sqrt{\frac{h}{a}}$ enters the expressions for the effective width (Eq. (12) and (16)). λ is proportional to the tangential shear forces T transmitted by the string (or in the actual case by the rib) to the shell (compare Eq. (6) and (7)). It takes into account the effect of the lag of the direct shear forces $N_{x\varphi}$ and $N_{\varphi x}$ on the effective width.

In summary, two effects govern the effective width of a cylindrical shell, the escaping in radial direction and the lag of the direct shear forces. In the T-Beam problem (flange plate is plane) the first factor does not enter provided the critical buckling stress is not exceeded.

---

*A boundary at a finite distance d may be considered with little error to be at infinity if $\beta d > 2.4$ (See Ref. (12), p. 25).

5. The Effective Width of Cylindrical Shells in Case the Radius of the Shell Increases to Infinity:

The question arises as to what the effective width of a cylindrical shell becomes if the radius "a" of the shell approaches infinity. Obviously the axis of the rib and the middle plane of the shell become straight and the effective width should be identical with the effective width of a flat plate reinforced by a rib (T-Beam). No difficulty exists in proving that the differential equations of the shell reduce to the differential equation of a flat plate if the radius "a" is increased to infinity.

Nevertheless this does not prove that the equations for the effective width of cylindrical shells given in the previous two chapters will check with those of the corresponding T-Beams. For Miesel's approximate solution (Eq. (3)), was used for the calculations and further simplifications were introduced (p. 9) in order to get expressions depending on two parameters λ and $\sqrt{ah}$ only.

The limiting process "a" $\to \infty$ was applied (Ref. 12) to the derived formulas for the effective width directly and these results were compared to the corresponding equations of a T-Beam with a straight axis. The effective width of ribbed cylindrical shells as presented herein reduces to the effective width of the corresponding T-Beams with a straight axis if the radius of the shell is increased to infinity. The check is complete from the practical point of view (differences of 0.5% and 1.4%), but it is not a

mathematically exact one. This is to be expected as an approximate solution (Eq. (3)) was used for the derivation of the effective width of cylindrical shells.

The close correspondence established between the two problems for the limiting case "a" $= \infty$ may be considered as a justification for the use of the approximate solution Eq. (3), in cases of very large a/h ratios.

Hence, the derived formulas for the effective width are not limited by a certain value of the radius "a", but are based on the general relations of the theory of elasticity. The stability of the shell and of the combination of the shell and the rib do limit the application, a problem which exists equally in the case of the T-Beam.

Part II

TESTS OF MODELS

by

Bruno Thürlimann, Rudolf O. Bereuter† and Bruce G. Johnston

INTRODUCTION

Part II

~~This report~~ presents results of tests of two models of thin cylindrical shells reinforced with ribs in the circumferential direction, simulating on a 1/30 scale typical cross-sectional proportions of thin shell hangar roof construction.* The circumferential length was sufficient to remove the center section from local end effects and at the same time permit the line of thrust during test to be near the shell, or on either side of it. Strains and deflections were measured and the results confirm the concept of an "effective width".

The theoretical investigation as presented in Part I extends the range of applicability of the test results. The test model consists of a pin ended curved beam-column, with the resultant direct forces P and bending moments M determinate at any section. (See Fig.10 and 11).

---

* In the present instance, based on concrete hangars of 300 foot span designed by the Roberts and Schaefer Engineering Co., for construction at Rapid City, South Dakota, and Limestone, Maine.

† Formerly Fritz Laboratory Special Research Assistant, now with Gebruder Sulzer A.G., Winterhur, Switzerland.

Description of Tests

Two series of models were tested and are referred to in the following as Model Series A and Model Series B. The dimensions are shown in Fig. 6 and Fig. 7. The difference in Model Series A and B consists essentially in a difference of distance between the two ribs, (12" and 18" respectively). Each model series included four different overhangs as seen in the above mentioned Fig.6 and Fig.7. The following is a table of the different tests:

Model No.	"A" Series Models Distance between ribs=12"		Model No.	"B" Series Models Distance between ribs = 18"	
A-1	Overhang	12"	B-1	Overhang	9"
A-2	"	6"	B-2	"	4.5"
A-3	"	3"	B-3	"	1.5"
A-4	"	0	B-4	"	0

Heavy plates were welded at each end of the test sections to permit variable location of the line of thrust in three different positions. The dimensions of the models were such that the disturbance at the springing line of the shell does not influence the middle part of the shell. The strain gages as shown in Fig.8 and 9, were placed at the middle to indicate the behavior due to the interaction of rib and shell only.

Ames Dials also shown in Fig. 9, were used to measure the deflections along the cross-section at the middle of the model.

The models were placed in a 60,000 pound Baldwin testing machine, and the load was applied through knife edges to the

model. The end block had three different grooves allowing three different eccentricities of the load (Fig. 6 and 7). Loading by means of grooves "1" caused a negative moment over the whole span of the model. For grooves "2" the end moments were negative, the moment in the middle positive. Positive moment over the whole span was provided by applying the load through grooves "3" (Fig. 10 and 11).

The following table explains the notation used for the tests. It will be referred to throughout the report.

NOTATION OF THE TESTS

	Overhang	Model	Load Case 1	Load Case 2	Load Case 3
Model A Rib distance 12"	12 in	A-1	A-11	A-12	A-13
	6	A-2	A-21	A-22	A-23
	3	A-3	A-31	A-32	A-33
	0	A-4	A-41	A-42	A-43
Model B Rib distance 18"	9 in	B-1	B-11	B-12	B-13
	4.5	B-2	B-21	B-22	B-23
	1.5	B-3	B-31	B-32	B-33
	0	B-4	B-41	B-42	B-43

Testing Procedure:

Coupon tests showed a yield stress $\sigma_y = 30{,}000$ for the steel used in making the models. The loads were chosen so as to stay in the elastic range, resulting in maximum loads of 5500 pounds for load case "1" and "3" and 10,000 pounds for load case "2".

Strain gage readings were taken at an initial load of 1,000 pounds and at the maximum load of 5,500 or 10,000 pounds, repeating the procedure once. Deflection readings were recorded at load increments of 1,000 pounds for case "1" and "3" and 2,000 pounds for case "2". This procedure was adopted to in-

vestigate the influence of the deflections on the magnitude of the moments. The measured values did not indicate any such influence, showing a perfect proportionality between load and deflection. An analytic study showed the increase in moment due to deflection to be about 3%, causing a non-linearity not readily detected in the experiments. The effect of deflections would have been greater had the loads been nearer to the values causing buckling of the panel.

Test Results:

Figure 12 shows the symbols used to represent moments, forces, and deflections. These differ somewhat from the notation in Part I but correspond to the notation commonly used in design of thin shell structures. From the recorded strains the moments and forces M_1, M_2, T_1 , T_2 were worked out. Typical results of T_2 and M_1 are plotted at the measurement locations in Fig. 13 and 14 for Model Series A and in Fig. 17 and 18 for Model Series B. T_1 and M_2 were very small and the results are omitted. In the same graphs the results of the analytical computations are shown by full lines. Only twelve out of the twenty-four tests are presented, these being typical of the results obtained.

Fig. 15 and 16 for Model Series A and Fig. 19 and 20 for Model Series B present the measured deflections plotted simultaneously with the calculated values.

DISCUSSION OF TEST RESULTS

The theoretical computations* were based on three simplifying assumptions:

*Complete test results and theoretical computations are on file at Fritz Engineering Laboratory, Lehigh University, Bethlehem, Pa.

1. Moment $M_2 = 0$ (See Fig. 12)
2. Poisson's ratio $\nu \neq 0$.
3. Torsional stiffness of the ribs = 0.

Forces and Moments:

The correspondence between the experimental and theoretical values of M_1 and T_2 is good. Some discrepancies appear to be caused by stress concentration, by local unevenness of the shell from manufacturing, and by the error in the strain recording system itself. The latter influence is of prime importance for the models under load case "3" (e.g. Test A-23, A-43, B-13) where the strains are of small magnitude. As confirmed experimentally, T_1 forces are insignificant and were not computed analytically.

M_2 moments (assumed zero in the analysis) have a similar distribution to the M_1 moments. In a cylindrical container under constant moments or shear forces along one edge, the M_2 moments are νM_1 (see Timoshenko "Plates and Shells" p. 391). In the present case the M_1 moments are not constant in circumferential direction, but the assumption $M_2 = \nu M_1$ is nevertheless in good agreement with the test results.

The influence of the torsional stiffness is insignificant for an overhang > 4.5". The portions of the shell on both sides of the rib are then very nearly self-balancing. The greatest effect occurs for zero overhang. As analytical studies showed, the torsional stiffness is of the order of the bending stiffness of the shell. Its consideration would greatly complicate the computation. The test results of the model A-4 and B-4 (Fig. 18) show that as a satisfactory approximation this influence

may be disregarded by assuming the torsional stiffness of the ribs to be zero.

Deflections:

Recalling that the deflection is a double integration of the moment over the whole structure, an error in the theoretical computation of the moments would result in greatly increased errors in computed deflections. Deflections are therefore very good criteria of the accuracy of a solution.

Fig. 15 and 16, Model Series A, and 19 and 20, Model Series B, show the experimental and theoretical deflections of rib and shell at the center of the span. The calculated rib deflections correspond fairly well with the test results. Considering the possible variation of the modulus of elasticity of about 3½%, the influence of the additional moments caused by the deflection of about 3%, and inaccuracies of manufacture, this represents a close correspondence. The shell deflections indicate the tendency of the shell to escape the direct forces T_2, bending outwards and inwards for compression and tension forces respectively.

Importance of the Overhang:

The importance of the overhang may be illustrated by the following comparison. The table shows the analytical results for Model A-3 and Model B-4 (Fig. 6 and 7) under load case 1.

	Model A-31	Model B-41
Rib distance	12"	18"
Overhang	2 @ 3"	0"
Overall width	18"	18"
T_2 max	-967.43 lb/in	-2109.27 lb/in
Deflection	0.1090 in.	0.1686 in.

Model A-3 has the same cross-sectional area as B-4, but the two ribs are placed three inches inside of the edges, whereas B-4 has the ribs on both ends. This difference of disposition of the ribs is responsible for an increase of $T_{2\ max}$ of 118% and of the deflection δ_{max} of 55%.

A sudden change in the behavior takes place for an overhang of about 3". If more than 3", the behavior approaches very quickly that for ∞ overhang. If less than 3", T_2 and δ increase rapidly to reach the values for 0 overhang. M_1 drops first but increases again approaching 0 overhang. The M_1 at the rib decreases, but the M_1 in between the ribs increases (See Fig. 13 and 18).

The effectiveness of the shell between the ribs, in participating with the ribs, is greatly increased by a small amount of overhang. The total effective shell area may increase by a factor of 4 as compared with the condition of no overhang. This may be important in increasing the buckling resistance of the rib and shell combination.

"Effective Width"

Since the experimentally determined values of both T_2 and the deflections agree well with the theoretically computed values, it follows that the theoretical effective widths calculated by the procedure presented in Part I are in good agreement with the test results.

Tests on models simulating to small scale (1:30) an entire hangar structure, consisting of three ribs and shell, have also been completed for the Roberts and Schaefer Co. The results of these tests also confirm the use of values of "effective width" as established by Part I of this report.

SUMMARY

An analytical and experimental study of thin cylindrical shells reinforced with ribs in the circumferential direction has been presented. Models with circumferential length sufficient to remove the center section from local end effects and at the same time permit the line of thrust during test to be near the shell, or on either side of it, were tested. Strains and deflections were measured and analytical expressions derived. The results confirm the concept of an "effective width" (participation of the shell in helping the ribs). The "effective width" is a function of $K\sqrt{ah}$, when a is the radius of the shell, h = thickness of the shell, and K is a constant depending on the restraint of the shell by the rib and upon the loading. Therefore it is allowable to assume an effective width and to calculate the ribs as arches independent of the shell.

ACKNOWLEDGEMENT

The report presents a part of the theoretical studies made during the course of a two years research program on shell arch roofs carried out at Fritz Engineering Laboratory, ~~of the~~ Department of Civil Engineering and Mechanics, Lehigh University, Bethlehem, Pennsylvania. Professor Wm. J. Eney is Head of the Department and Director of the Laboratory. Mr. Lynn S. Beedle, Assistant to the Director, and Mr. Kenneth R. Harpel, Laboratory Foreman, gave valuable assistance throughout the investigation.

Roberts and Schaefer ~~Engineering~~ Company, Chicago, Illinois, was sponsor of the research program. Many thanks are expressed to Mr. J.E. Kalinka, Executive Vice-President of the Company, and to

Mr. Robert Zaborowski, ~~Principal Engineer at~~ Manager of the New York Office, who was representing the company, for their continued assistance. The many suggestions received from Mr. A. Tedesko, O. Gruenwald, W. A. Renner and P. Rongved, all of Roberts and Schaefer Company, during several meetings are sincerely acknowledged.

NOTATIONS

Roman Alphabet

a	radius of the shell
b	effective width
C	constant of integration, Eq. (3) or Table A
e	base of natural logarithm
E	modulus of elasticity
h	thickness of the shell
H	symbol for any force, moment etc., of the shell
$\overline{H}$	coefficient depending on the quantity H under consideration, Table A
k, k'	coefficients defined in Table A
k_1, k_2	coefficients defined in Table A
$K(\beta l, \lambda)$	function of the two parameters βl and λ, used for the effective width
l	length of the shell in axial direction
L	span of T-Beam or half-wave length of the string force S
M_x or M_1	bending moment in axial plane per unit width of the shell ~~in axial direction~~
M_φ or M_2	bending moment in circumferential plane per unit width of the shell in circumferential direction
$M_{x\varphi}$, $M_{\varphi x}$	twisting moments per unit width of the

	shell
n	n^{th} term of a Fourier series (number of complete cosine-waves of the string force S around the cylinder)
N_x	direct force per unit width of the shell in axial direction
N_φ	direct force per unit width of the shell in circumferential direction
$N_{x\varphi}$, $N_{\varphi x}$	direct shear forces per unit width of the shell
p, p_o	distributed line load.
Q_x	normal shear force per unit width of the shell acting on a face x = constant
Q_φ	normal shear force per unit width of the shell acting on a face φ= constant
S	string force S defined by Eq. (1)
$S_n(x)$	string force at a distance x in the case of the n^{th} harmonic, defined by Eq. (5)
T	total shear force per unit width of shell in circumferential direction, Eq. (6)
T_1 , T_2	Corespond in Part II to N_x and N_ϕ in Part I
u	displacement in axial direction, Fig. 3
v	displacement in circumferential direction, Fig. 3
w	displacement in radial direction, positive outward, Fig. 3

x	coordinate of the shell in axial direction
y	coordinate of the T-Beam in direction of its axis

Greek Alphabet

α	angle corresponding to a half-wave of the string force
β	shell coefficient, depending on the thickness h and the radius "a" of the shell, Fig. 5
λ	parameter of the effective width, see Table A
μ_1, μ_2	numerical coefficients, defined in Table A
ν	Poisson's ratio
σ	stress
σ_x	bending stress in axial direction
σ_φ	direct stress in circumferential direction
$\tau_{x\varphi}$	shear stress of the shell on a cut x = constant in circumferential direction
τ_{yx}	shear stress in the flange of a T-Beam
φ	angular coordinate of the shell in circumferential direction
ξ	dimensionless coordinate in x-direction ($\xi = \frac{x}{a}$)
ψ	angle, constant of integration, Eq. (3) or Table A

LIST OF REFERENCES

(1) v.Karman, Th. "Die mittragende Breite". Festschrift Aug. Föppls, Springer, Berlin, 1924, p. 114.

(2) Metzer, W. "Die mittragende Breite". Luftfahrtforschung, vol. 4, 1929, p. 1.

(3) Timoshenko, S. "Theory of Elasticity". McGraw-Hill, New York, 1934, p. 156.

(4) Chwalla, E. "Die Formeln zur Berechnung der voll mittragenden Breite dünner Gurt- und Rippenplatten". Der Stahlbau, vol. 9, 1936, p. 73.

(5) Raithel, W. "The Determination of the Effective Width of Wide-Flanged Beams". Techn. Report Nr.61, Ordnance Research and Development Division, 1949.

(6) Finsterwalder, U. "Die querversteiften zylindrischen Schalengewölbe mit kreissegmentförmigem Querschnitt". Ingenieur Archiv, vol. 4, 1933, p. 43.

(7) Bleich, H. "Die Spannungsverteilung in den Gurtungen gekrümmter Stäbe mit T- und I -förmigem Querschnitt". Der Stahlbau, vol.6, 1933, p. 3, or Navy Department, Translation 228, 1950.

(8) v.Karman, Th. "Analysis of Some Typical Thin-Walled Structures". Transaction ASME, Aeronautical Eng., vol. 55, 1933, p. 155.

(9) Flügge, W. "Statik und Dynamik der Schalen", Springer, Berlin, 1934, or Edwards Brothers, Inc., Ann Arbor, 1943.

(10) Miesel, K. "Ueber die Festigkeit von Kreiszylinderschalen bei nicht-achsensymmetrischer Belastung". Ingenieur Archiv, vol. 1, 1929, p. 22.

(11) Girkmann, K. "Flächentragwerke". Springer, Wien, 1946.

(12) Thürlimann, B. "The Effective Width of Circular Cylindrical Shells Reinforced by Ribs". PhD-Dissertation, Lehigh University, 1950.

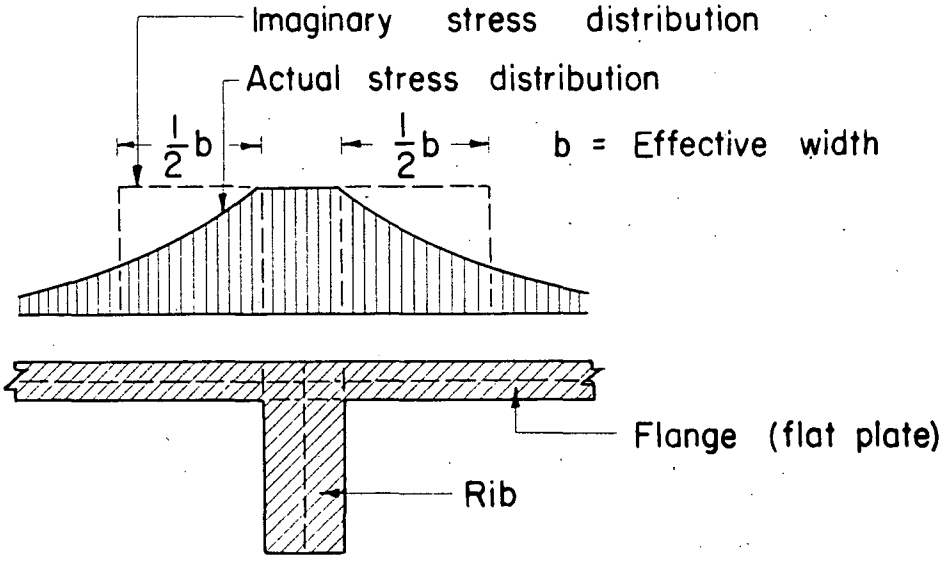

T - Beam

Fig. 1

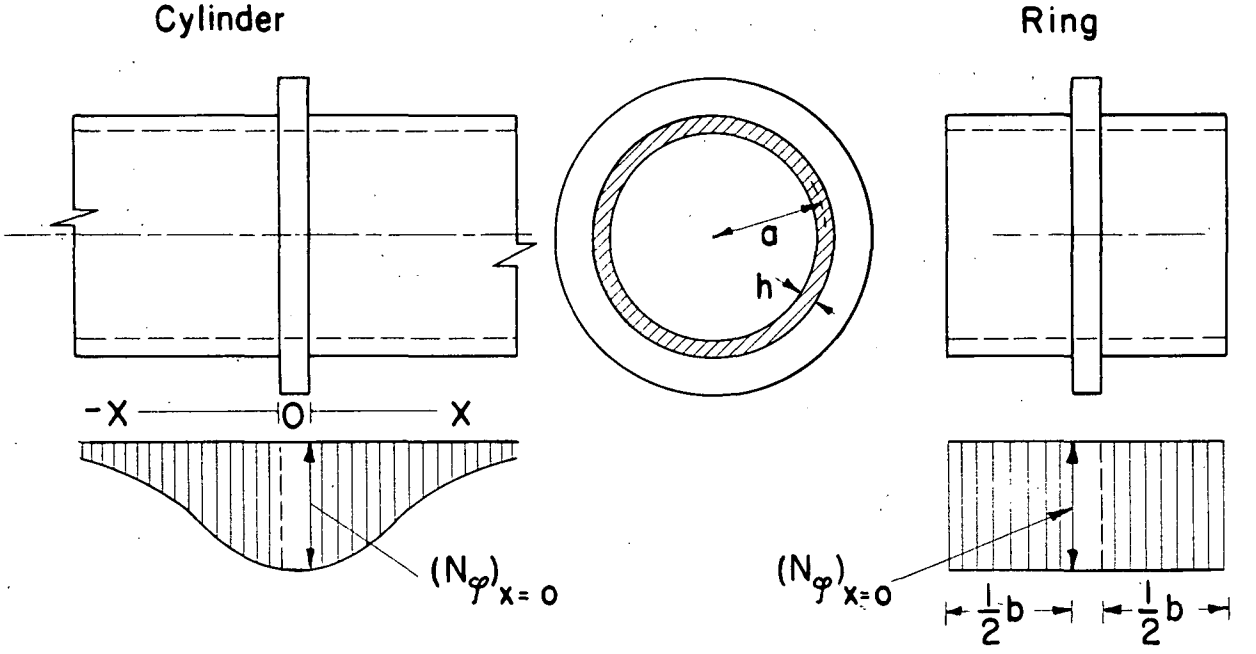

Fig. 2

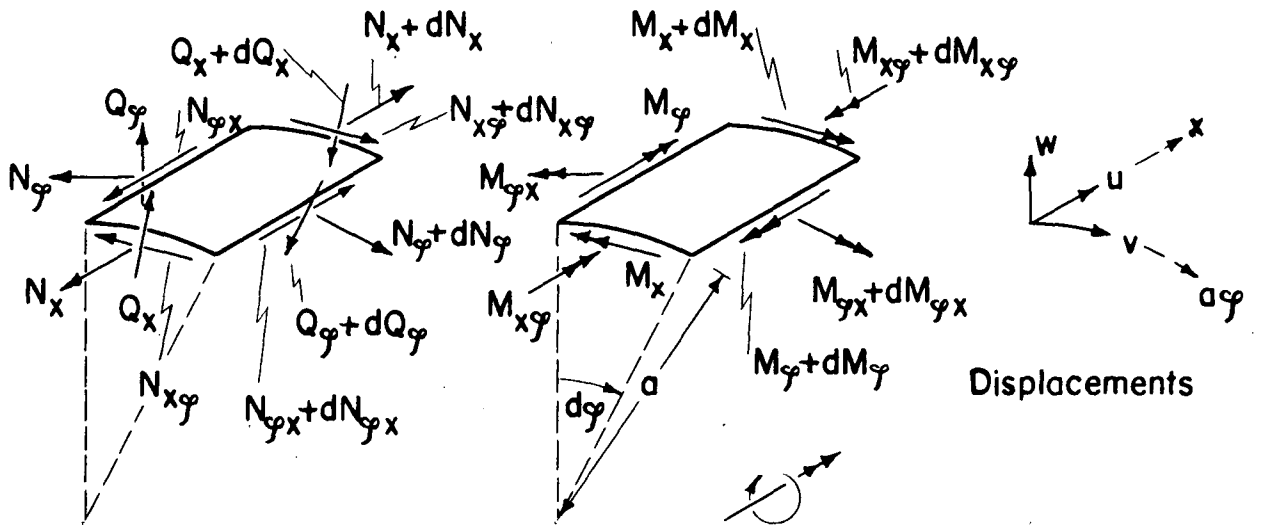

Fig. 3

Variation of String Force S

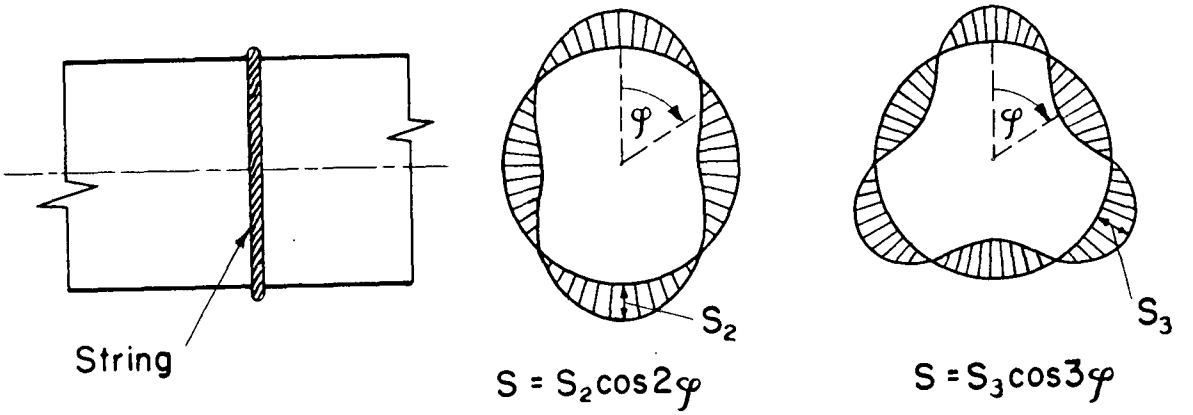

Fig. 4

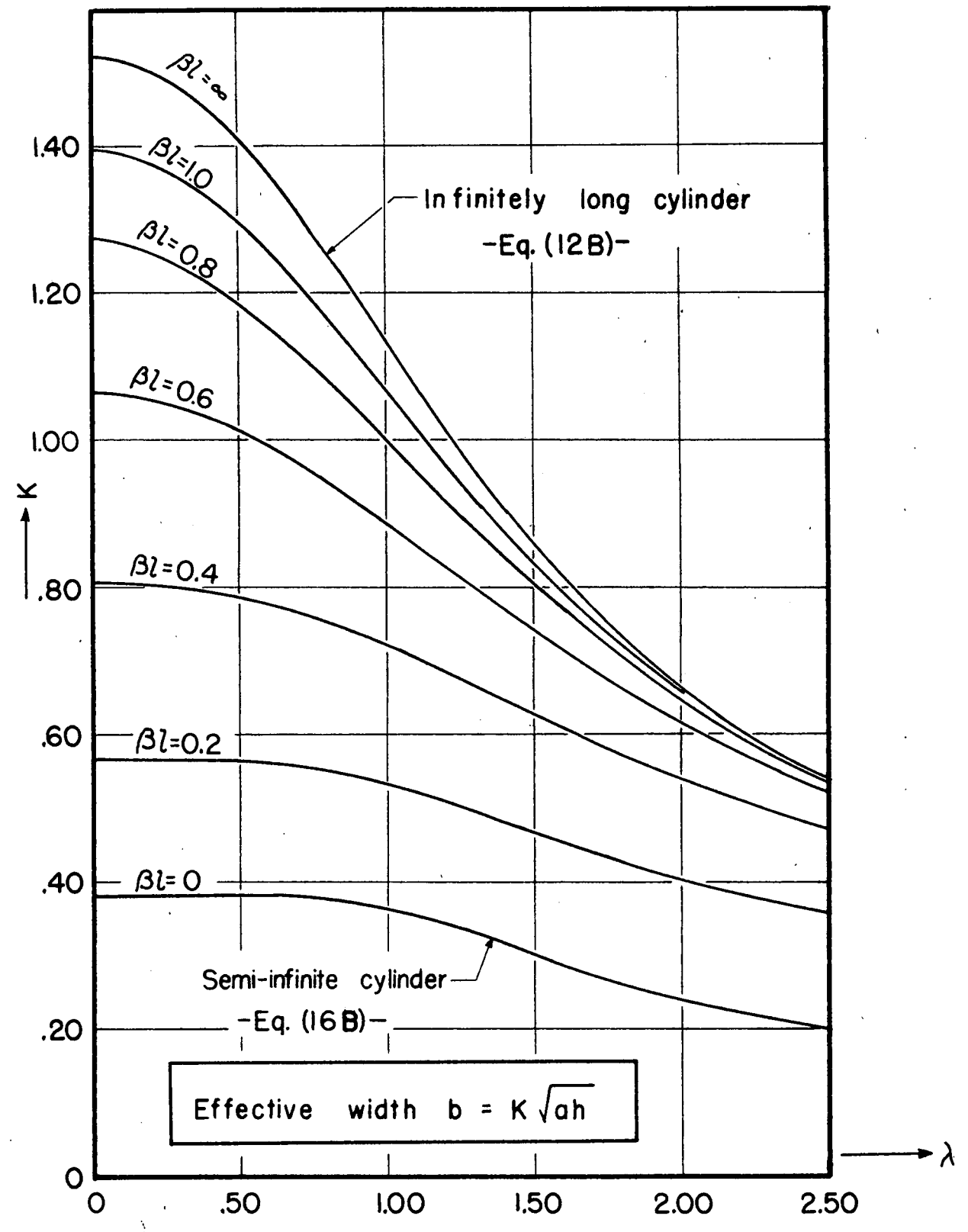

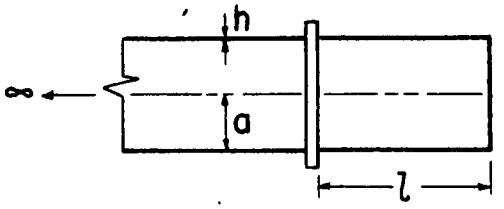

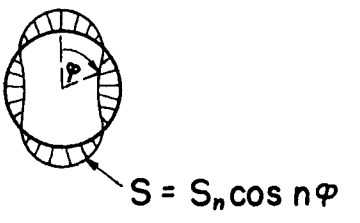

$$\lambda = n\sqrt{\frac{h}{a}}$$

$$\beta = \frac{1.3161}{\sqrt{ah}}$$

Fig. 5

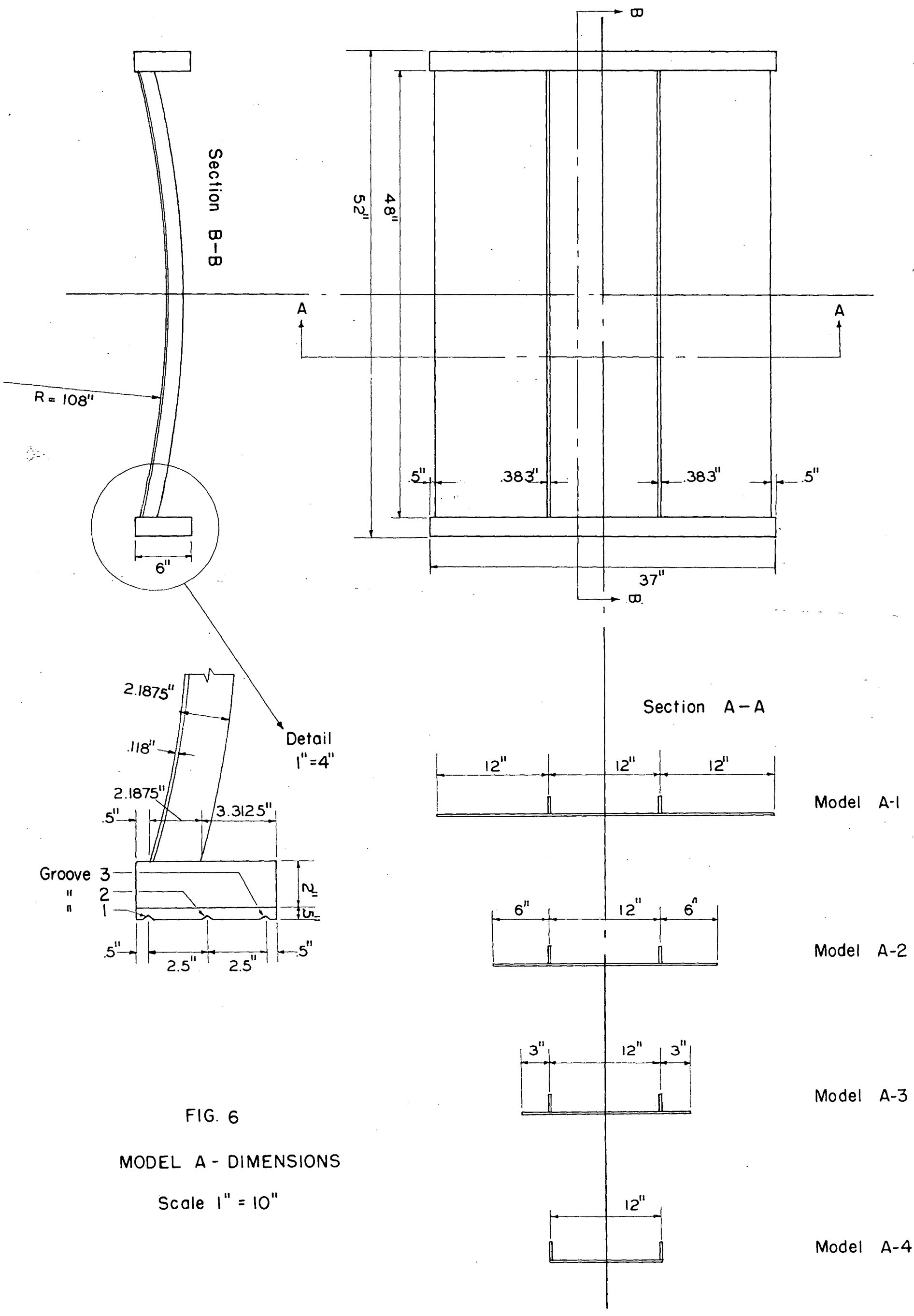

FIG. 6

MODEL A - DIMENSIONS

Scale 1" = 10"

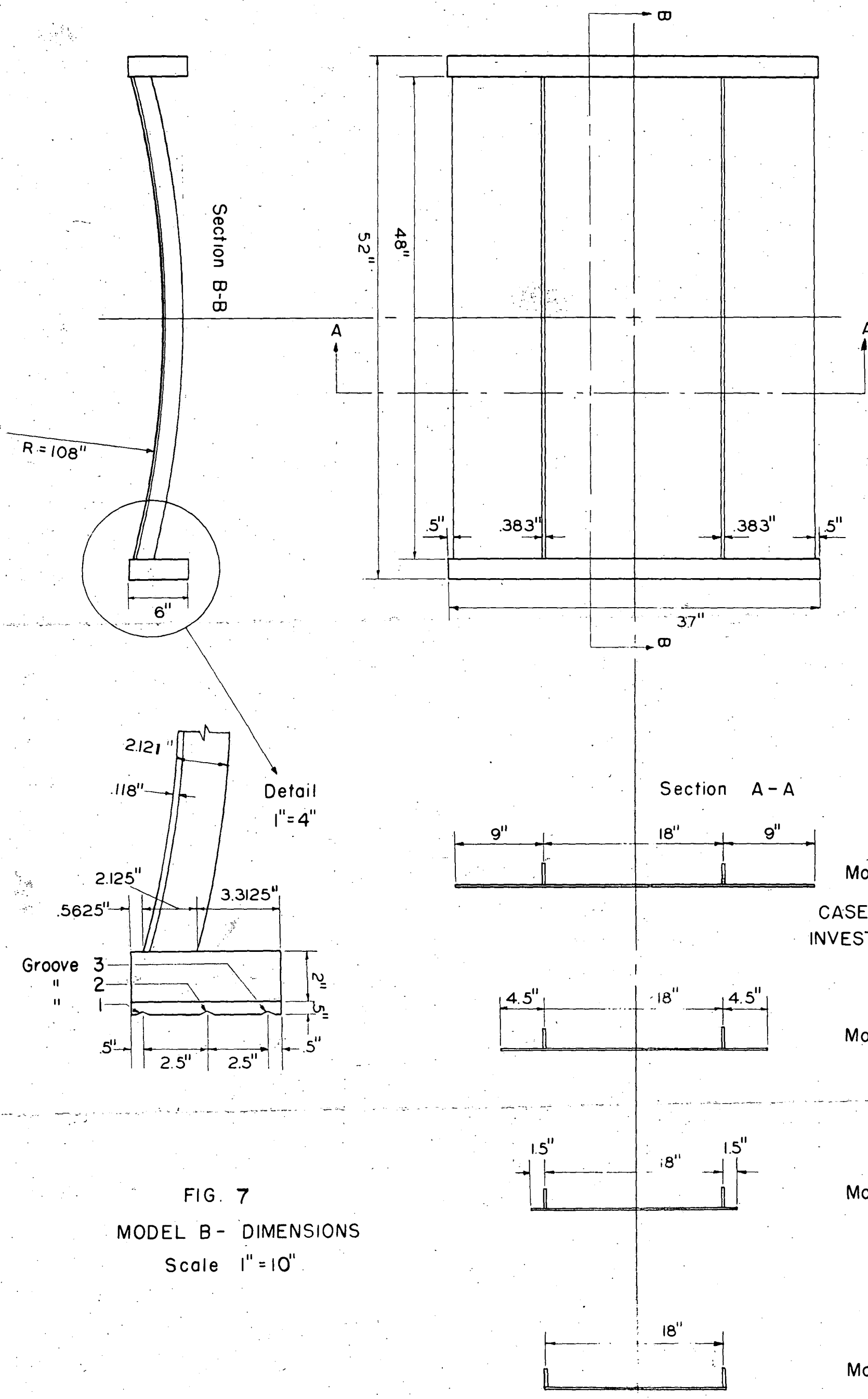

FIG. 7

MODEL B- DIMENSIONS

Scale 1" = 10"

- Fig. 8 -

Model A-2, rib side, showing strain gage arrangement.

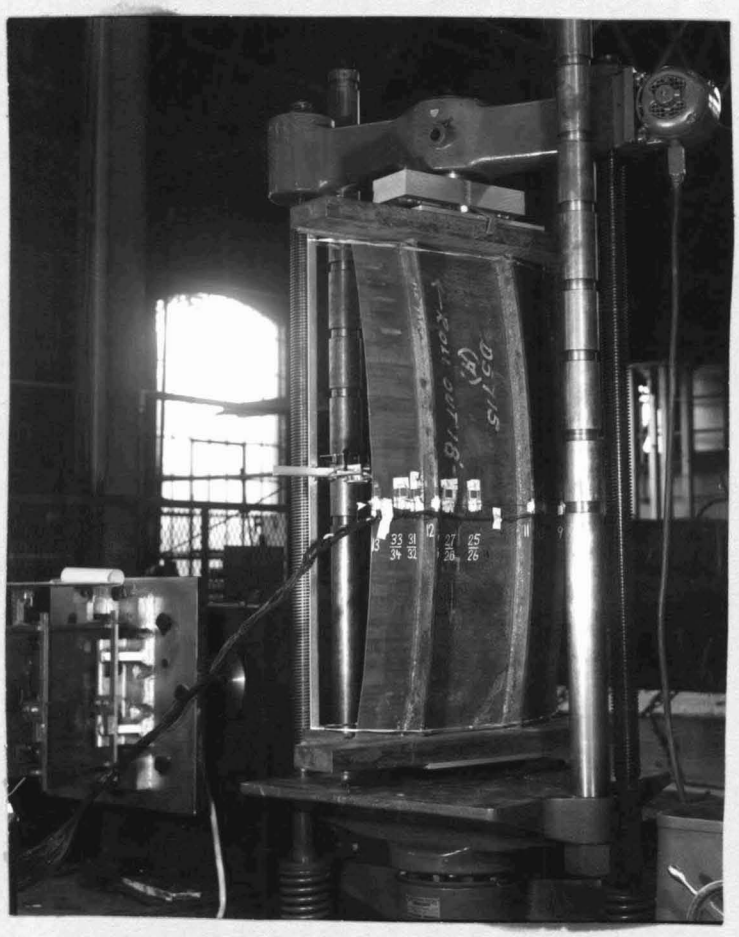

- Fig. 9 -

Dial gage arrangement.

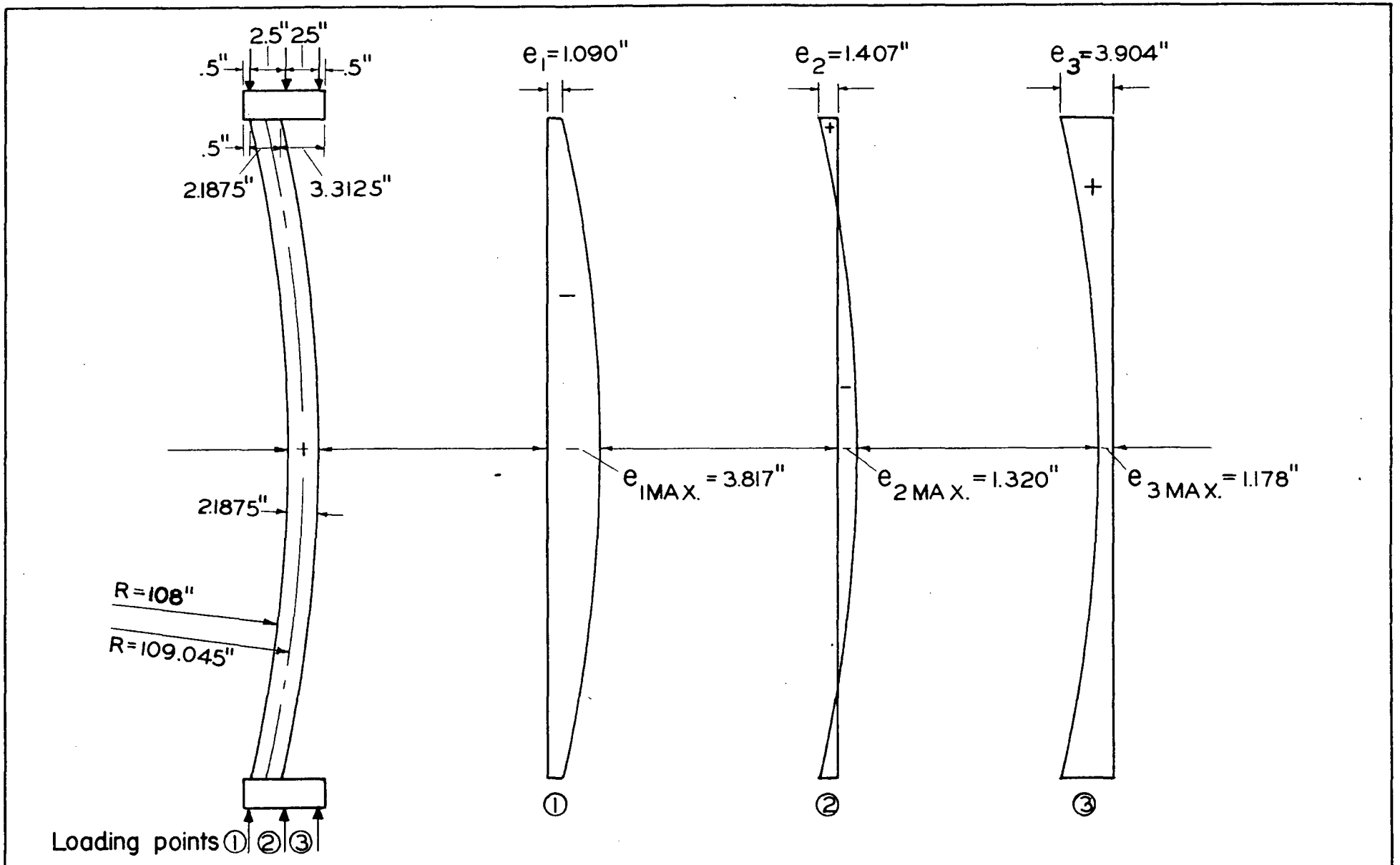

MODEL A – TOTAL MOMENT DIAGRAMS ALONG CENTERLINE OF RIBS

Fig. 10

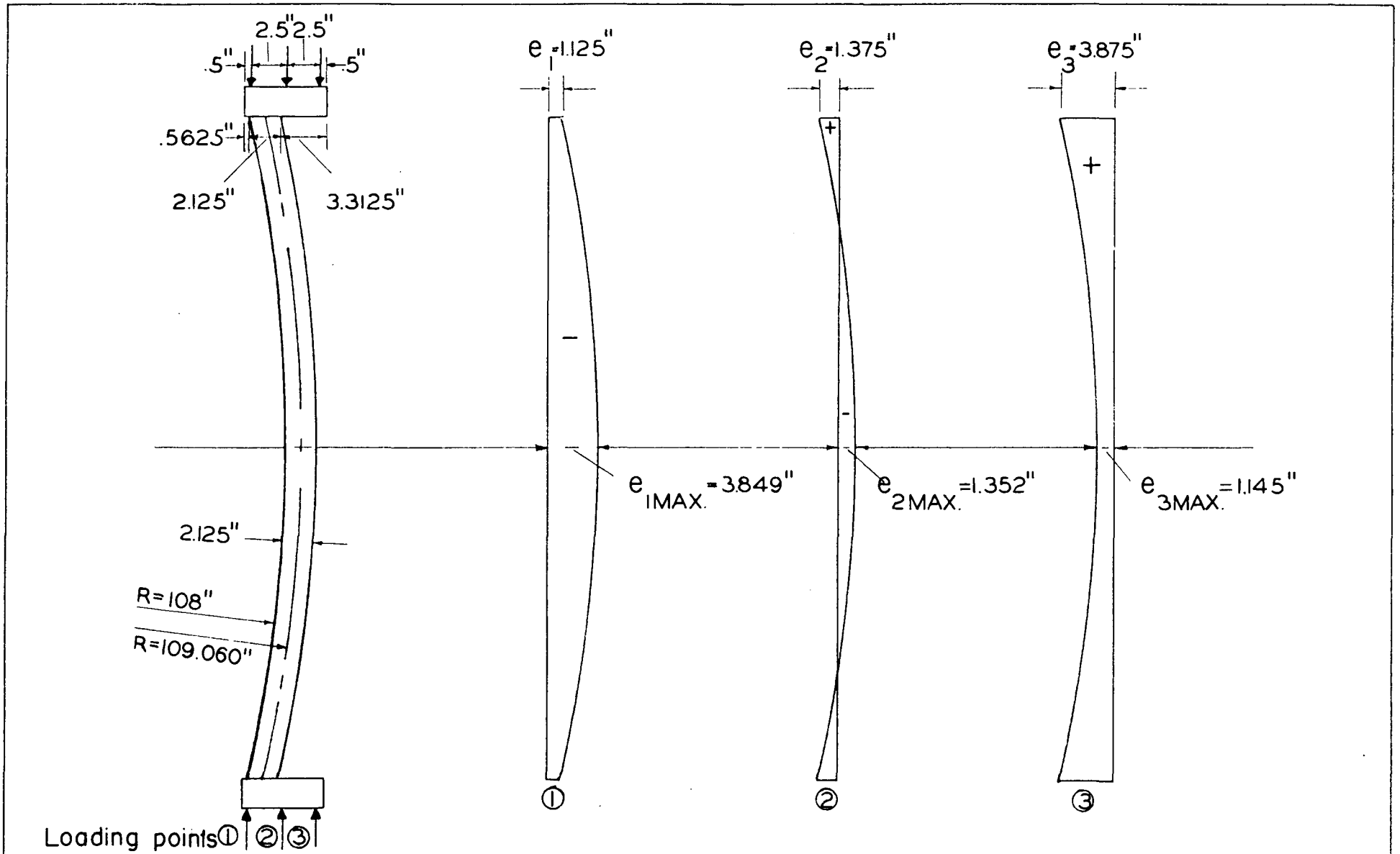

MODEL B – TOTAL MOMENT DIAGRAMS ALONG CENTERLINE OF RIBS

Fig. 11

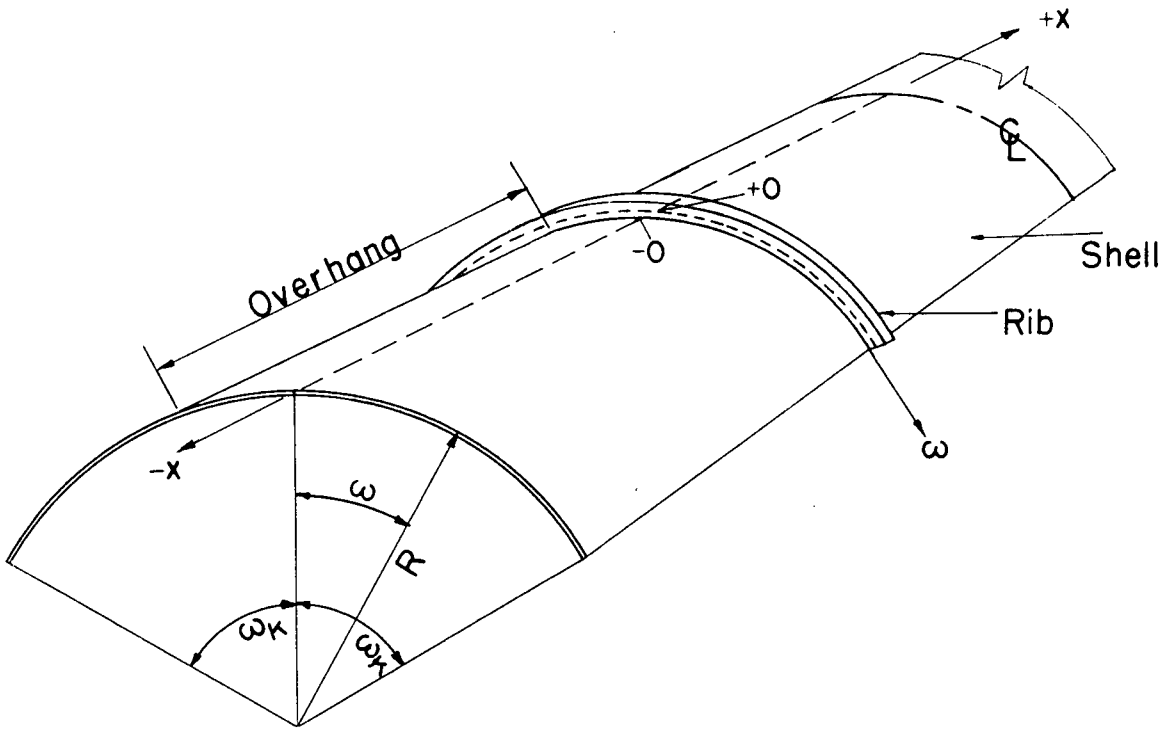

Coordinate System

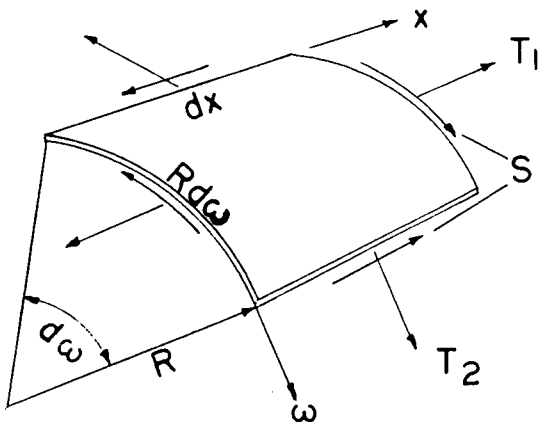

Membrane Forces

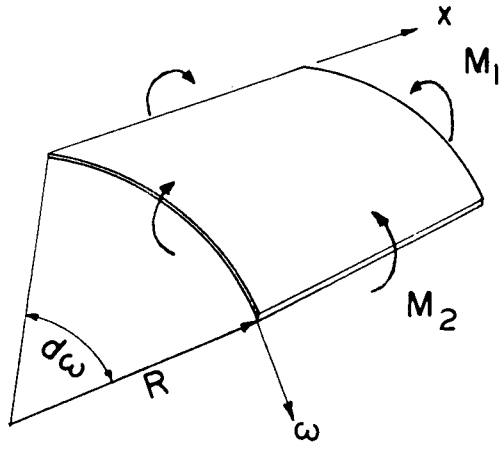

Bending Moments

FIG. 12 - COORDINATE SYSTEM AND SYMBOLS

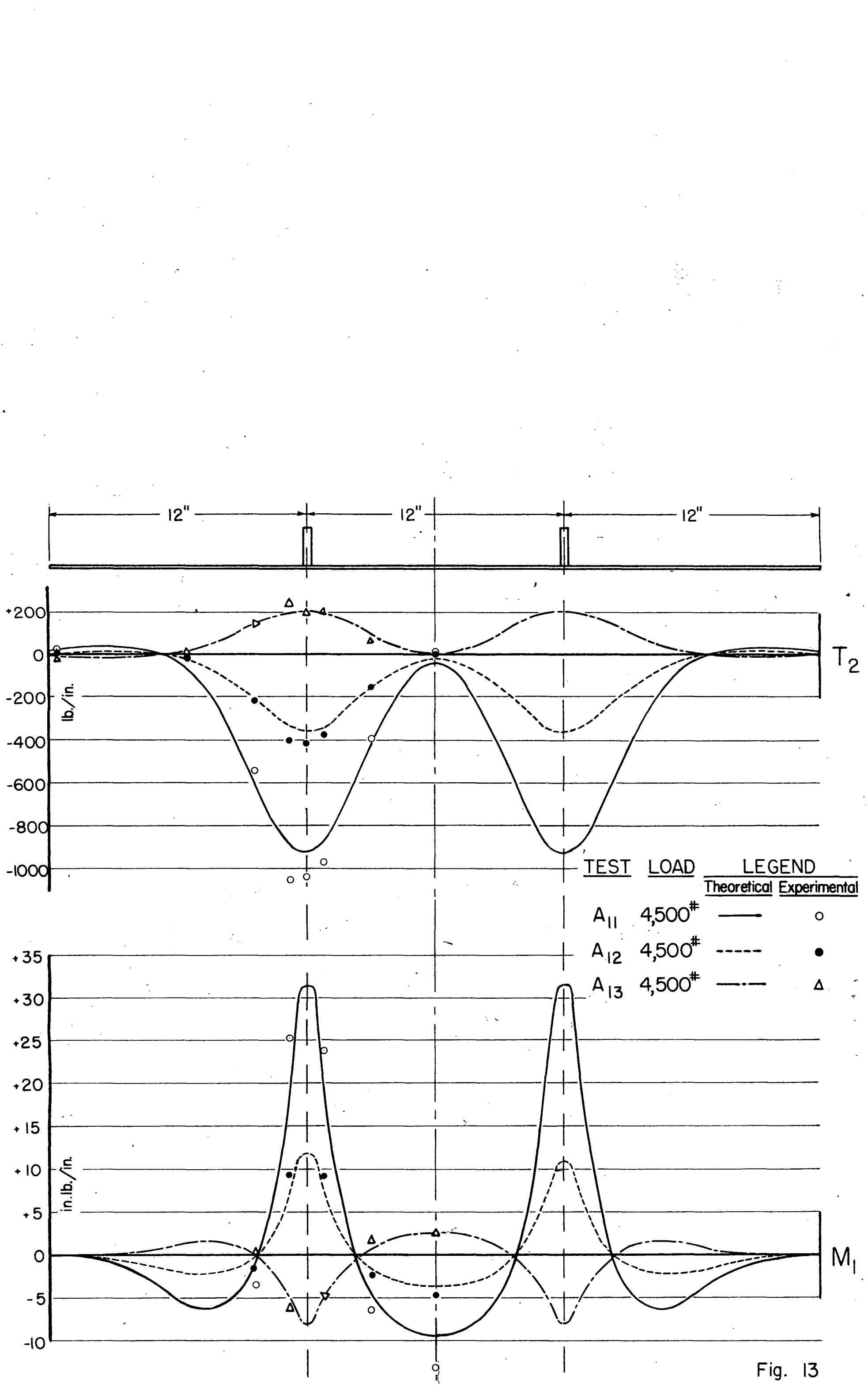
12"
12"
12"
+200
0
-200
-400
-600
-800
-1000
lb./in.
T_2
TEST LOAD
LEGEND
Theoretical
Experimental
A_{11} 4,500#
A_{12} 4,500#
A_{13} 4,500#
+35
+30
+25
+20
+15
+10
+5
0
-5
-10
in.lb./in.
M_1

Fig. 13

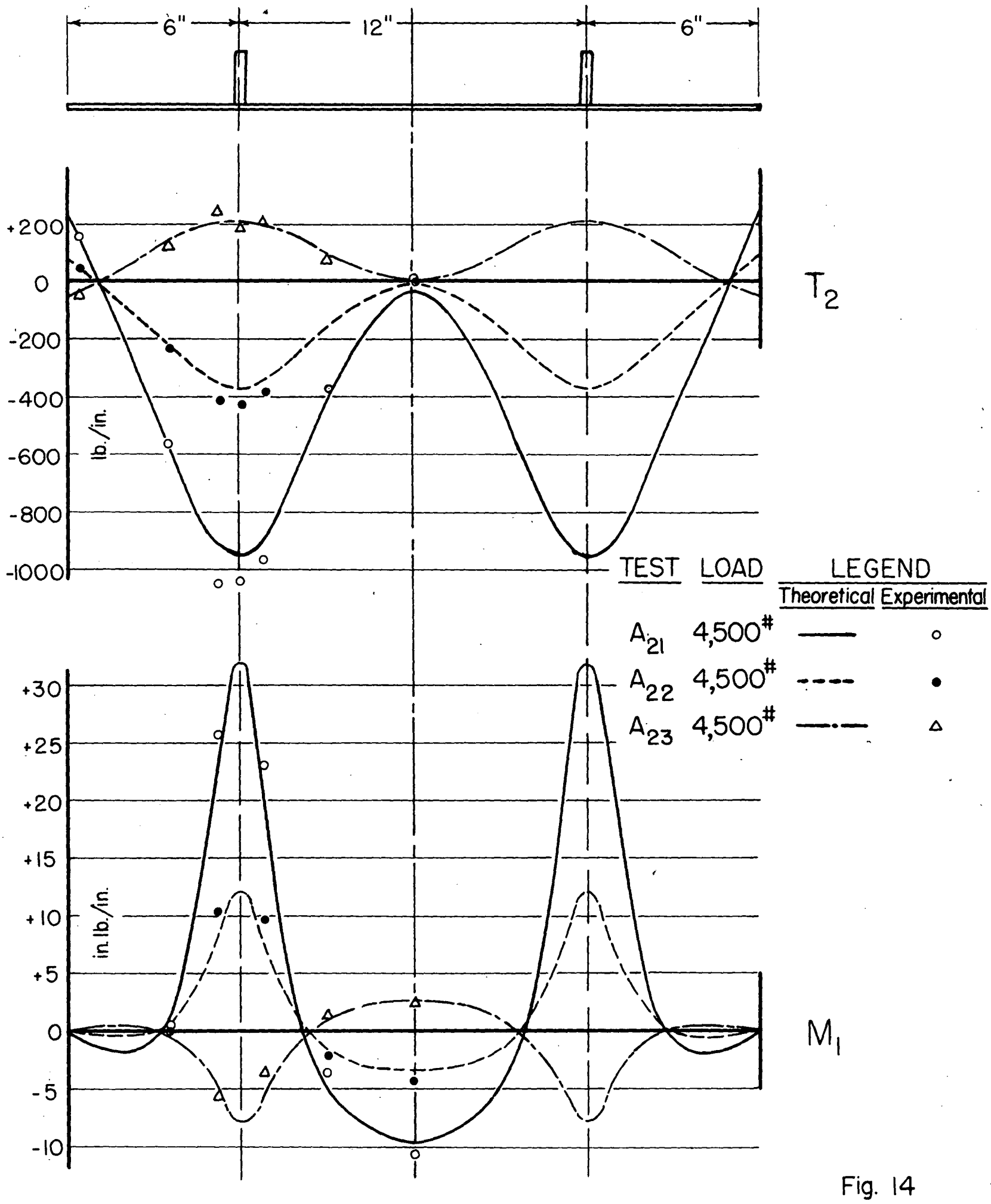
6"
12"
6"
+200
0
-200
-400
-600
-800
-1000
lb./in.
T_2
TEST LOAD
LEGEND
Theoretical Experimental
A_{21} 4,500#
A_{22} 4,500#
A_{23} 4,500#
+30
+25
+20
+15
+10
+5
0
-5
-10
in.lb./in.
M_1

Fig. 14

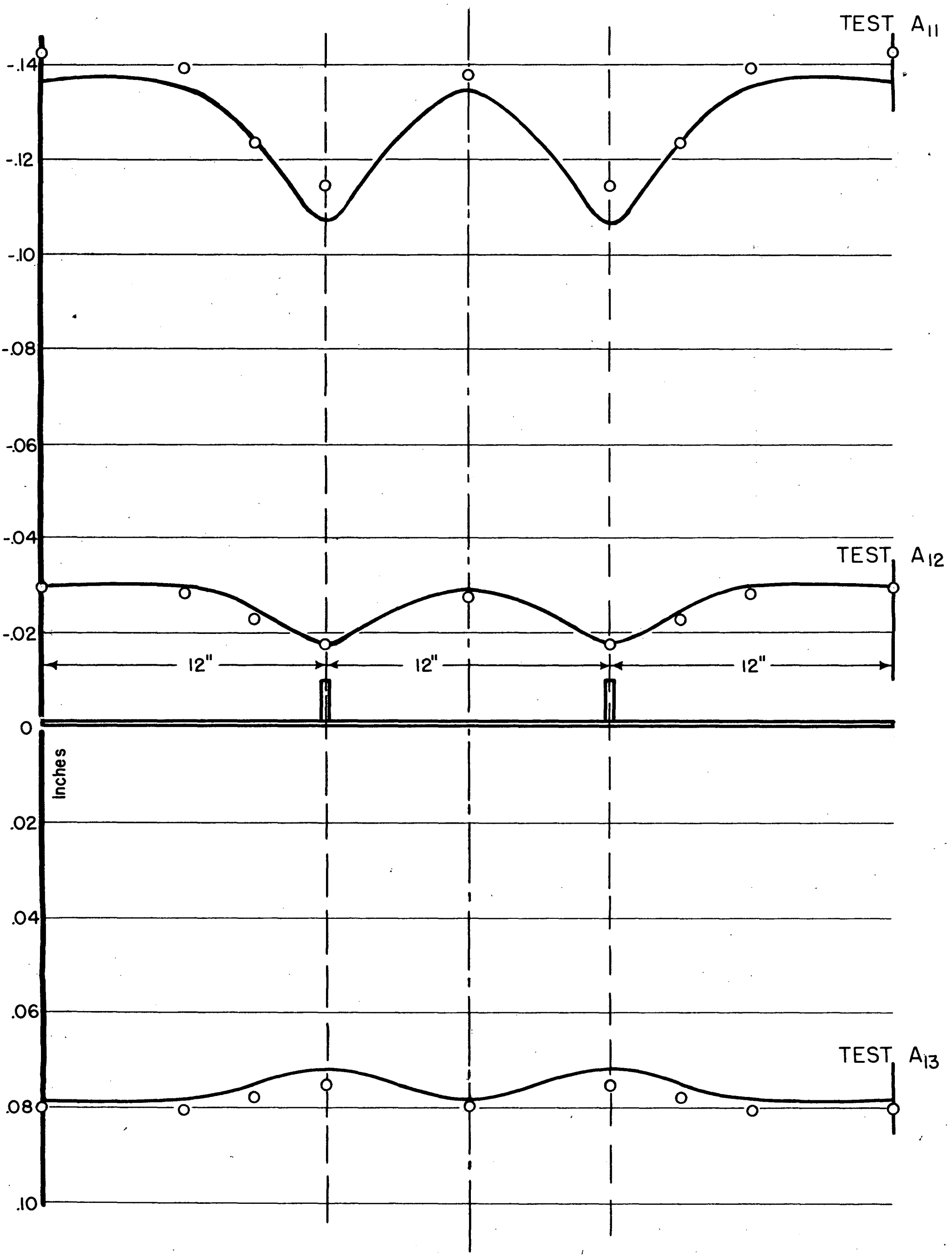

DEFLECTION MODEL A_1
THEORETICAL —
EXPERIMENTAL ○

Fig. 15

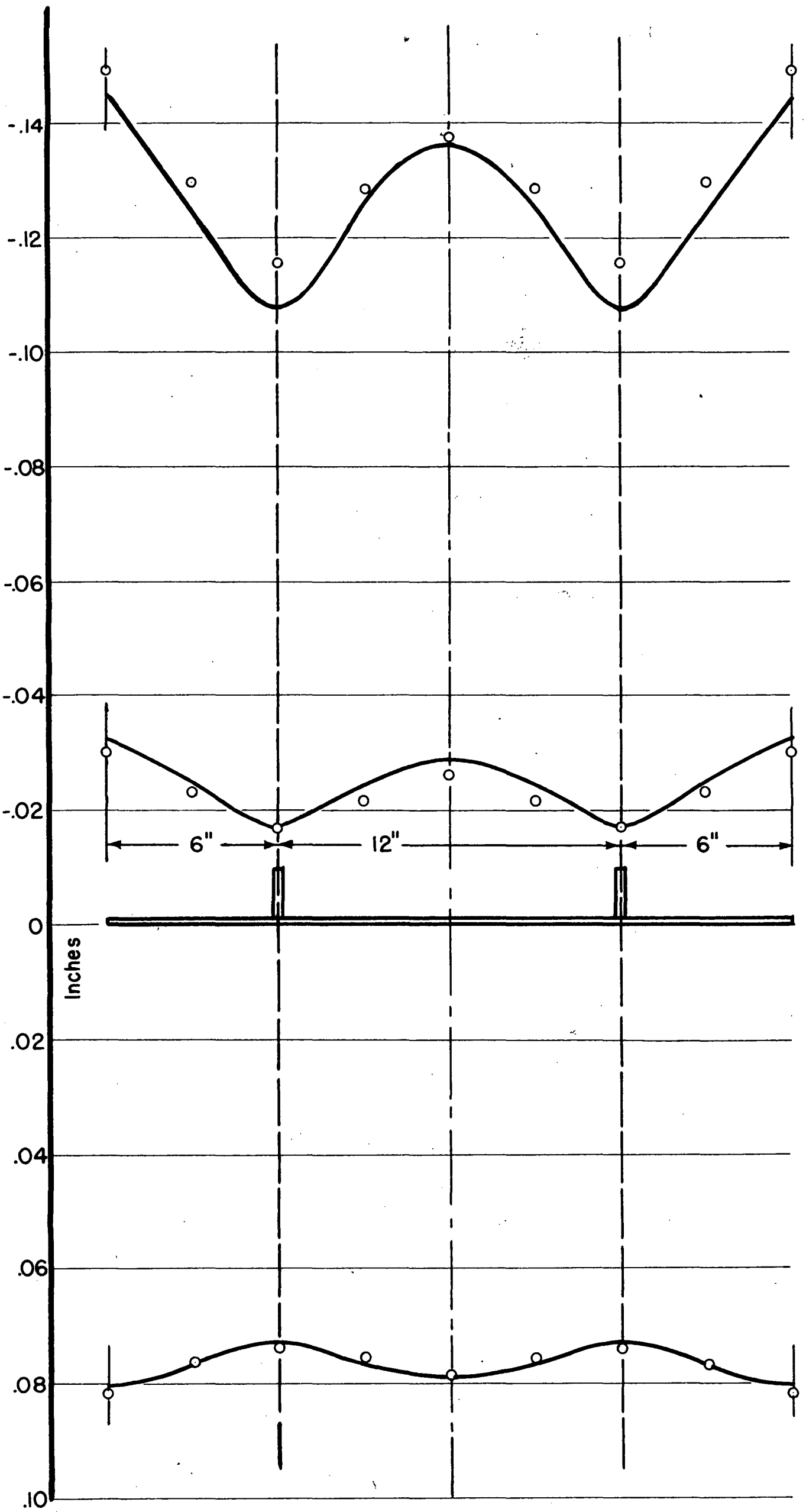

DEFLECTION MODEL A_2

THEORETICAL —

EXPERIMENTAL ○

Fig. 16

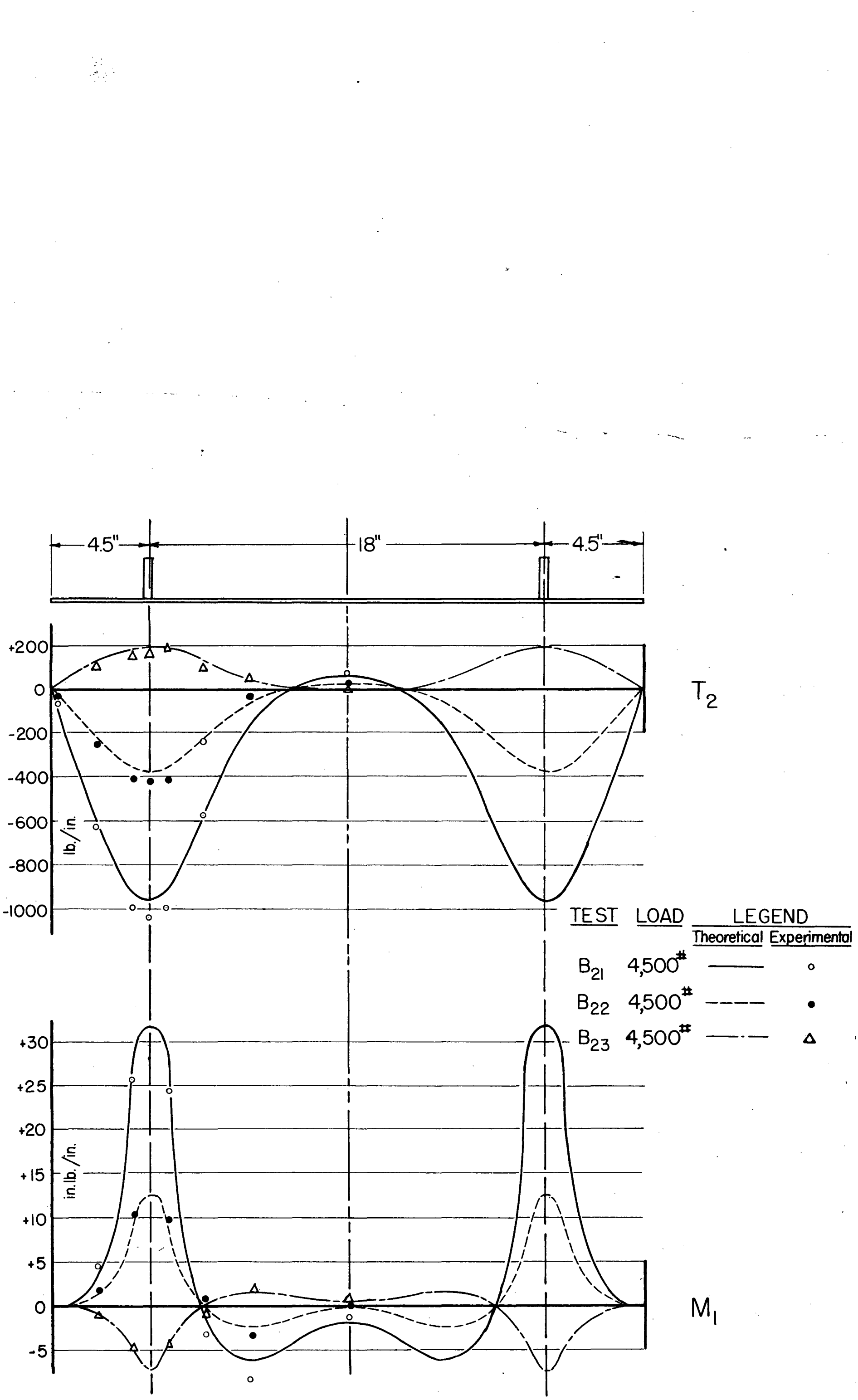
4.5"
18"
4.5"
+200
0
-200
-400
-600
-800
-1000
lb./in.
T_2
TEST LOAD
LEGEND
Theoretical Experimental
B_{21} 4,500# ——— o
B_{22} 4,500# – – – •
B_{23} 4,500# —·— Δ
+30
+25
+20
+15
+10
+5
0
-5
in.lb./in.
M_1

Fig. 17

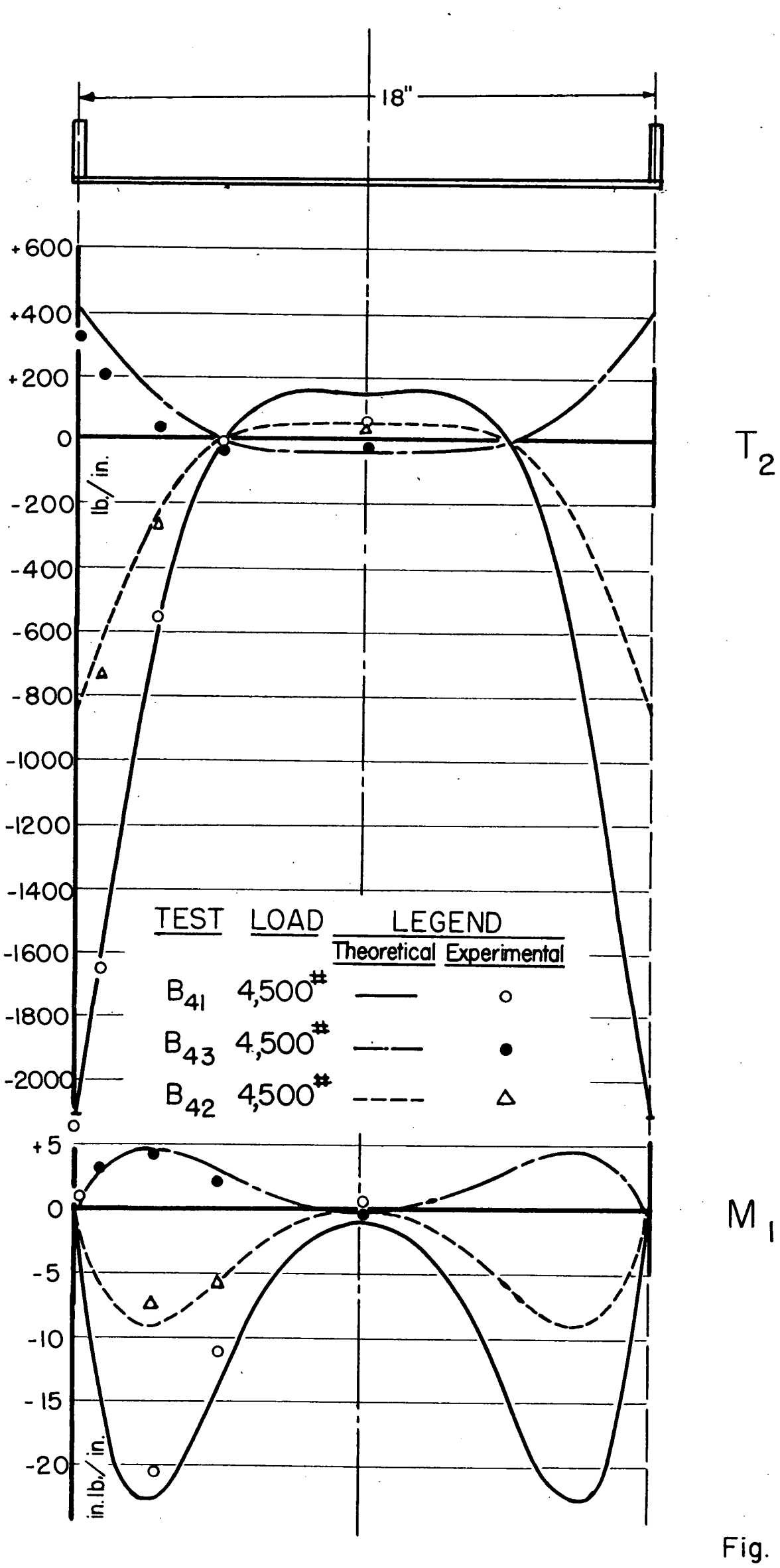
18"
+600
+400
+200
0
-200
-400
-600
-800
-1000
-1200
-1400
-1600
-1800
-2000
lb./in.
TEST LOAD
LEGEND
Theoretical Experimental
B41 4,500#
B43 4,500#
B42 4,500#
+5
0
-5
-10
-15
-20
in.lb./in.

T_2

M_1

Fig. 18

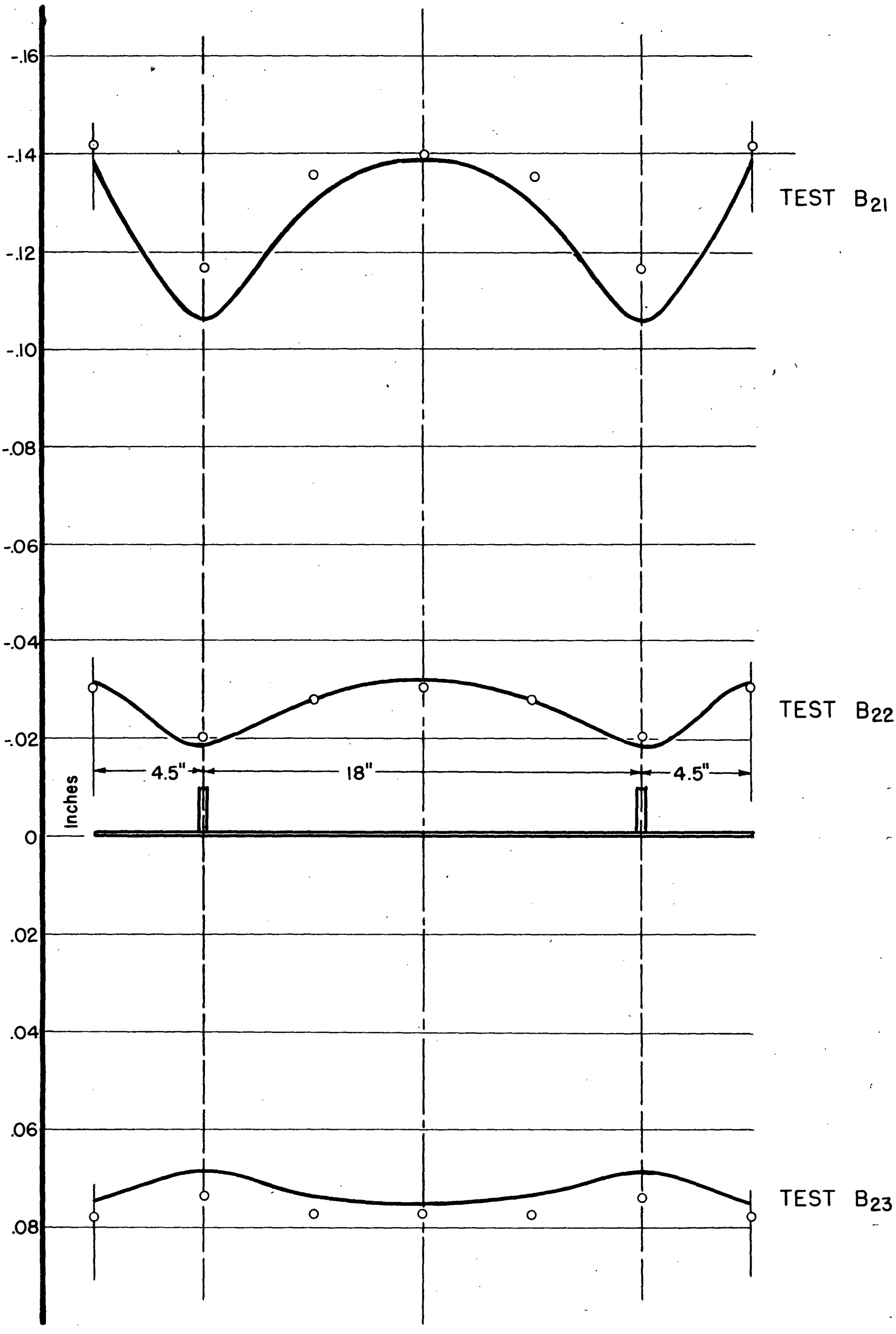

DEFLECTION MODEL B_2
THEORETICAL—
EXPERIMENTAL○

Fig. 19

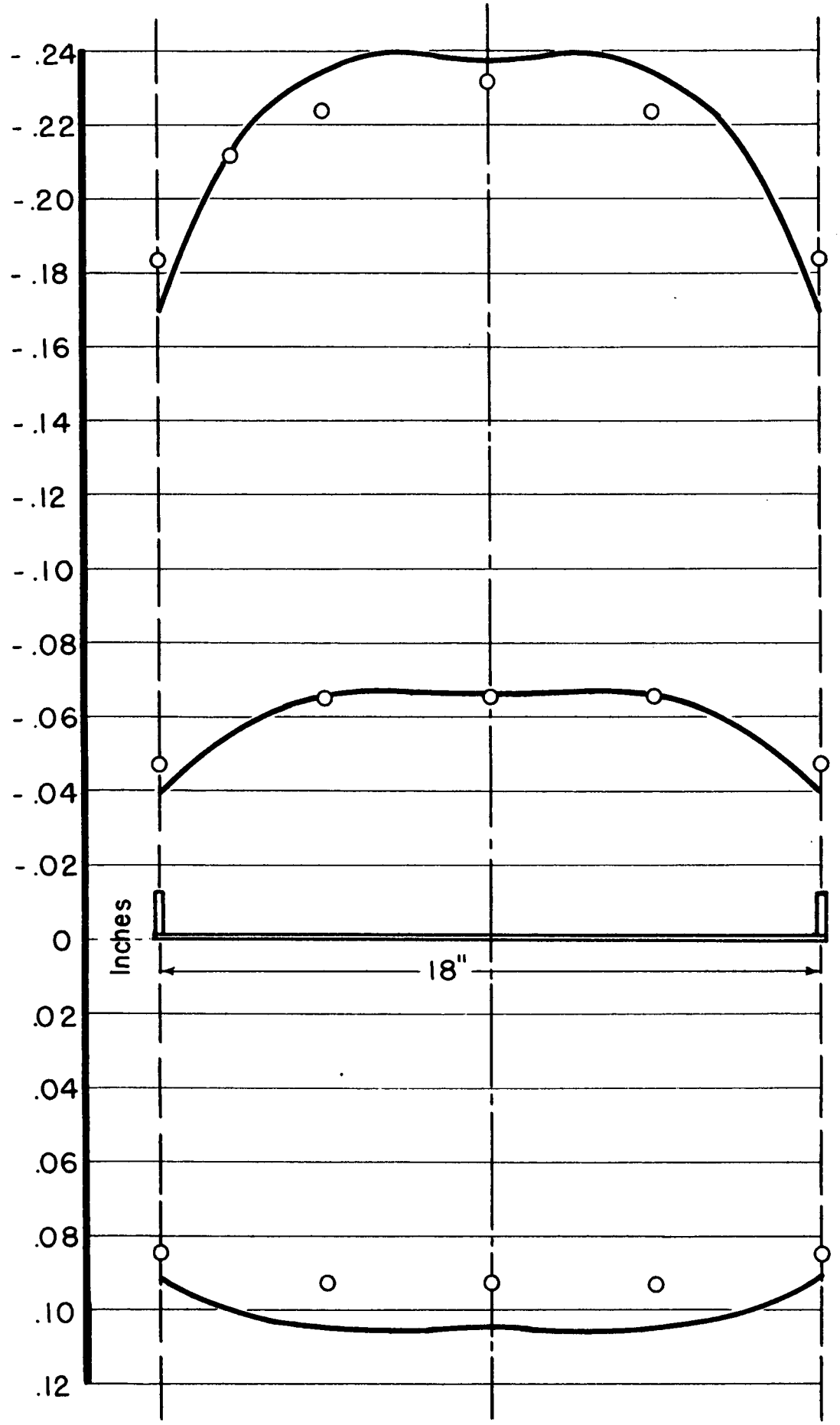

DEFLECTION MODEL B_4

THEORETICAL —

EXPERIMENTAL ○

Fig. 20